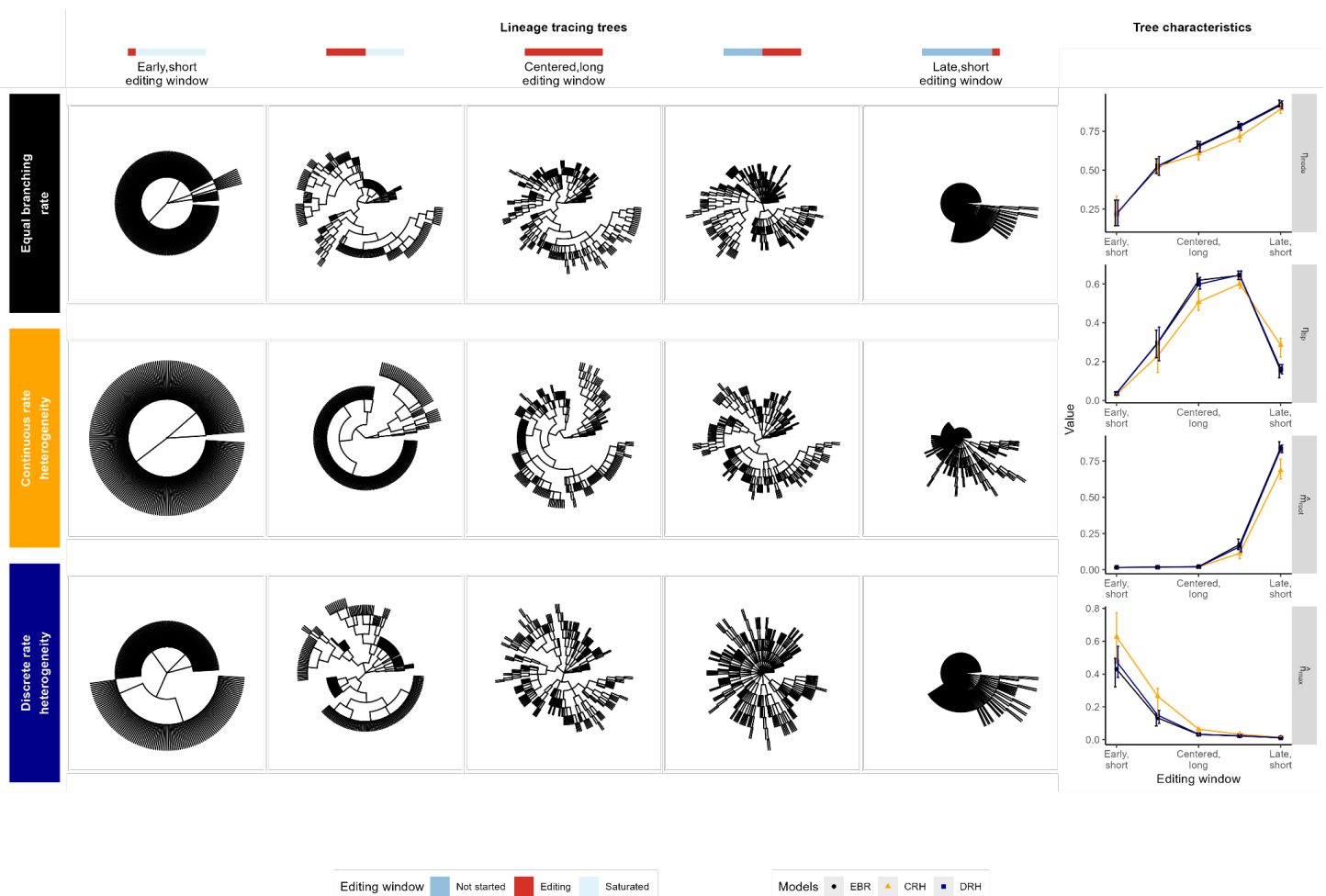
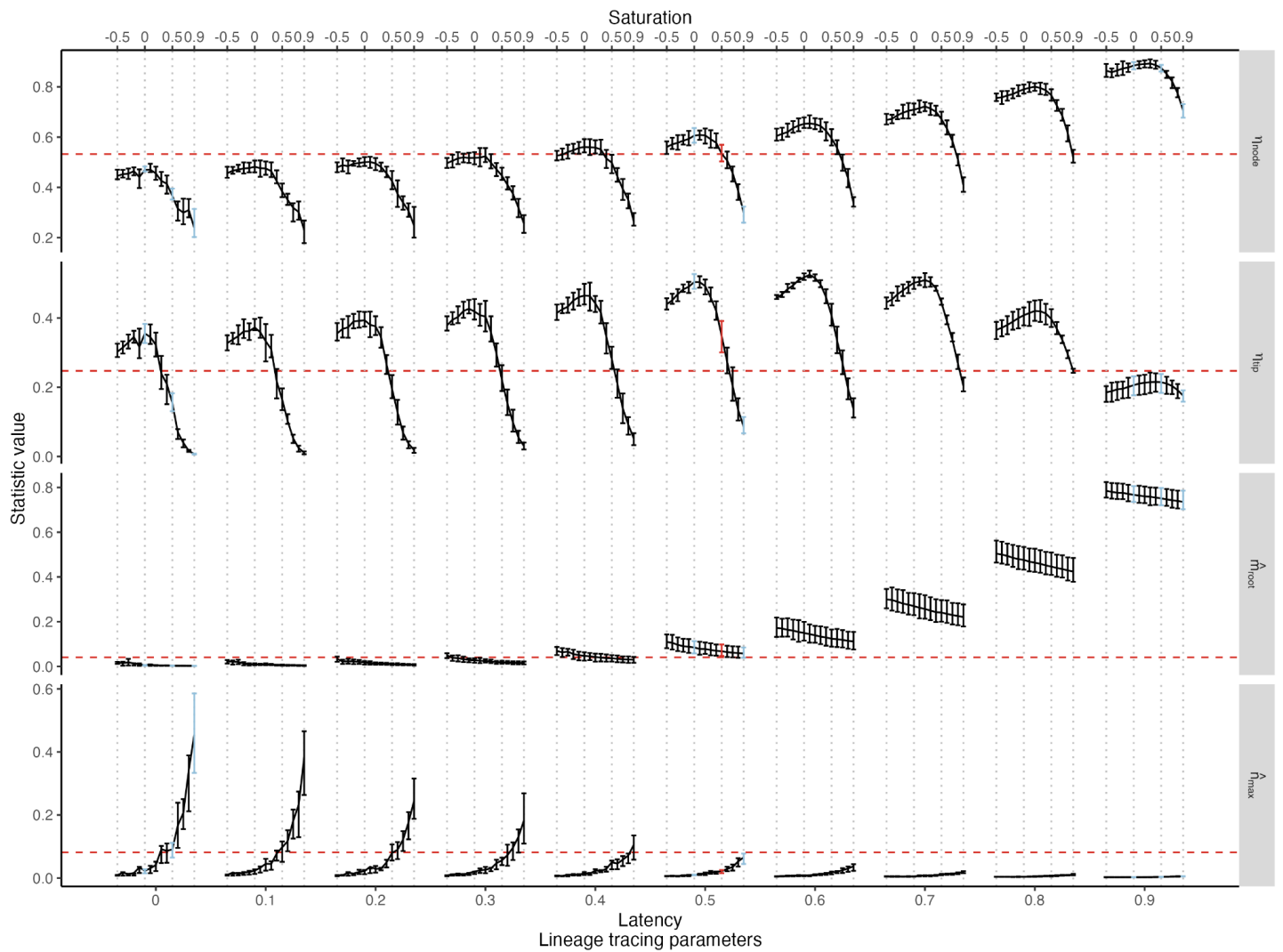


## Supplementary Figures



**Figure S1.**

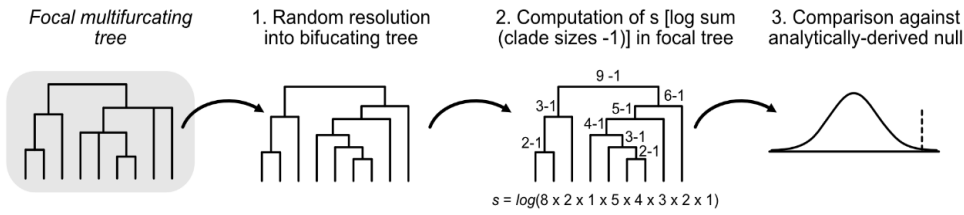
Timing and length of the lineage tracing window distorts the shape and characteristics of phylogenetic trees. Left: tree shapes under EBR, CRH ( $c = 1$ ) and DRH (fold change = 2, transition rate = 1), shown in rows top to bottom, and under different lineage tracing settings, shown in columns. Editing windows shown are left:  $t_{lag}^* = 0$ ,  $r_{edit}^* = 0.9$ ; left-middle:  $t_{lag}^* = 0$ ,  $r_{edit}^* = 0.5$ ; middle:  $t_{lag}^* = 0$ ,  $r_{edit}^* = 0$ ; right-middle:  $t_{lag}^* = 0.5$ ,  $r_{edit}^* = 0$ ; right:  $t_{lag}^* = 0.9$ ,  $r_{edit}^* = 0$ . All trees show  $N = 250$ . Summary statistics ( $\eta_{node}$ ,  $\eta_{tip}$ ,  $\hat{m}_{root}$ ,  $\hat{n}_{max}$ ) vary under different lineage tracing parameters; error bars represent interquartile range over 100 simulated trees. For summary statistics under a full combinatorial array of  $t_{lag}^*$  and  $r_{edit}^*$ , see Figure S2.



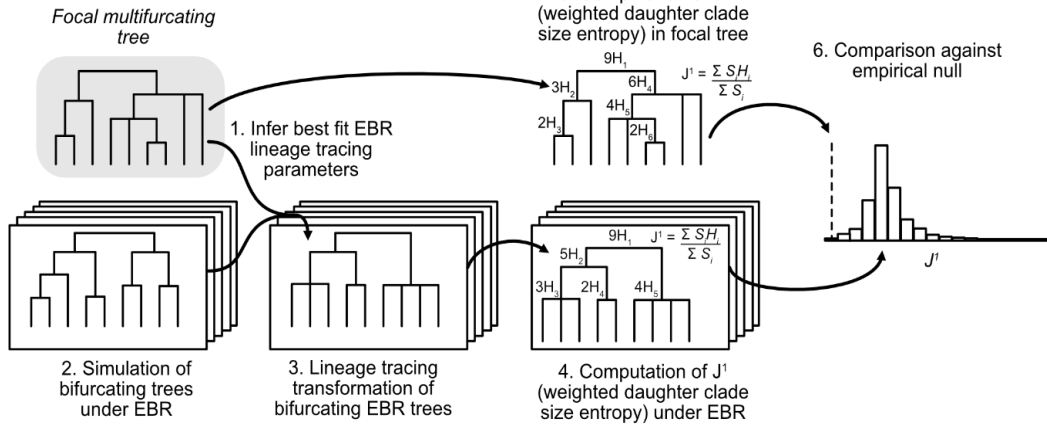
**Figure S2.**

Tree summary statistics across diverse lineage tracing settings. The four tree statistics ( $\eta_{node}, \eta_{tip}, \hat{\eta}_{root}, \hat{\eta}_{max}$ ) are computed for 20 trees each with all combinations of lineage tracing latencies  $t_{lag}^* = 0, 0.1, \dots, 0.9$  and  $r_{edit}^* = -0.5, -0.4, \dots, 0.4, 0.5$ . Bars represent interquartile range, and a curve interconnects all means within a latency parameter. We compare these values to the tree statistics of mouse M2 from Simeonov et al (15) plotted in red, dashed horizontal lines. We highlight the lineage tracing parameters that were used in the central power analysis (Figures 2, 3, S4) in red ( $t_{lag}^* = 0.5, r_{edit}^* = 0.5$ ). We selected this set of parameters as the ones that best matched  $\eta_{node}$  to the M2 tree. We highlight the additional lineage tracing parameters that were used in the robustness power analysis (Figure S7) in light blue.

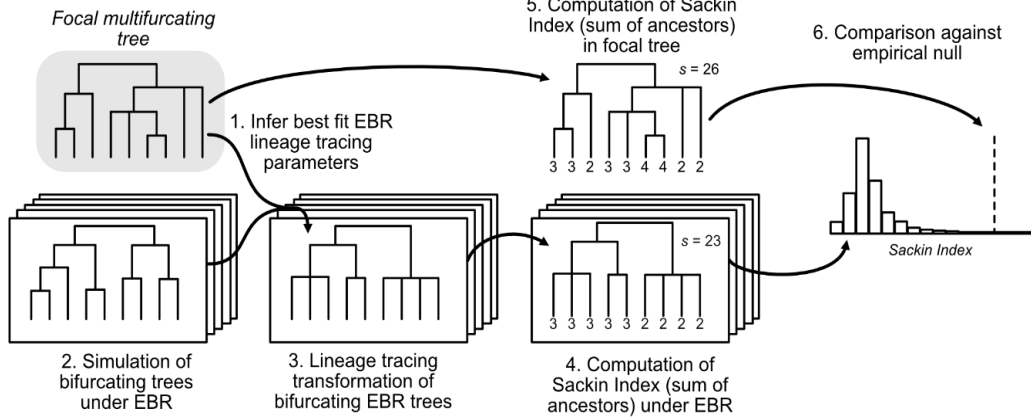
**$\hat{s}$  statistic**



**$J^1$  Index**



**Sackin Index**



**Uniform Nodal Probability (UnifNP)**

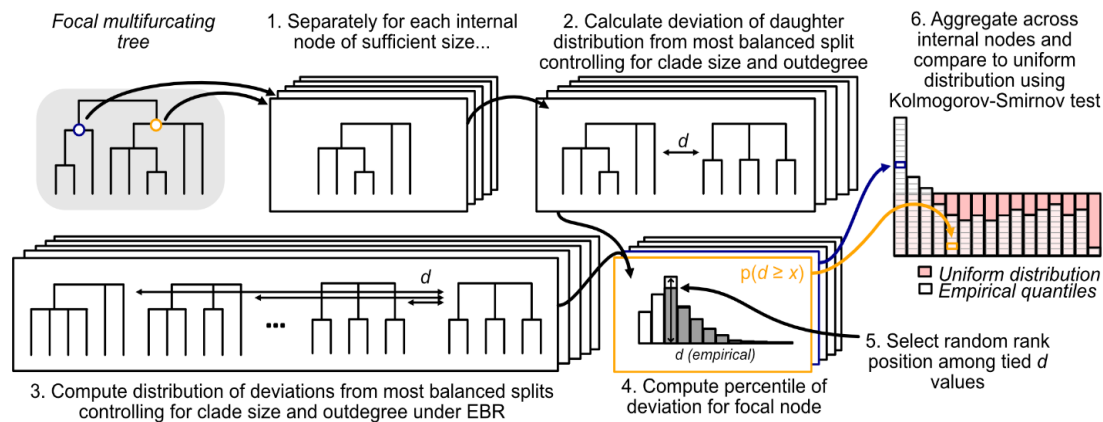
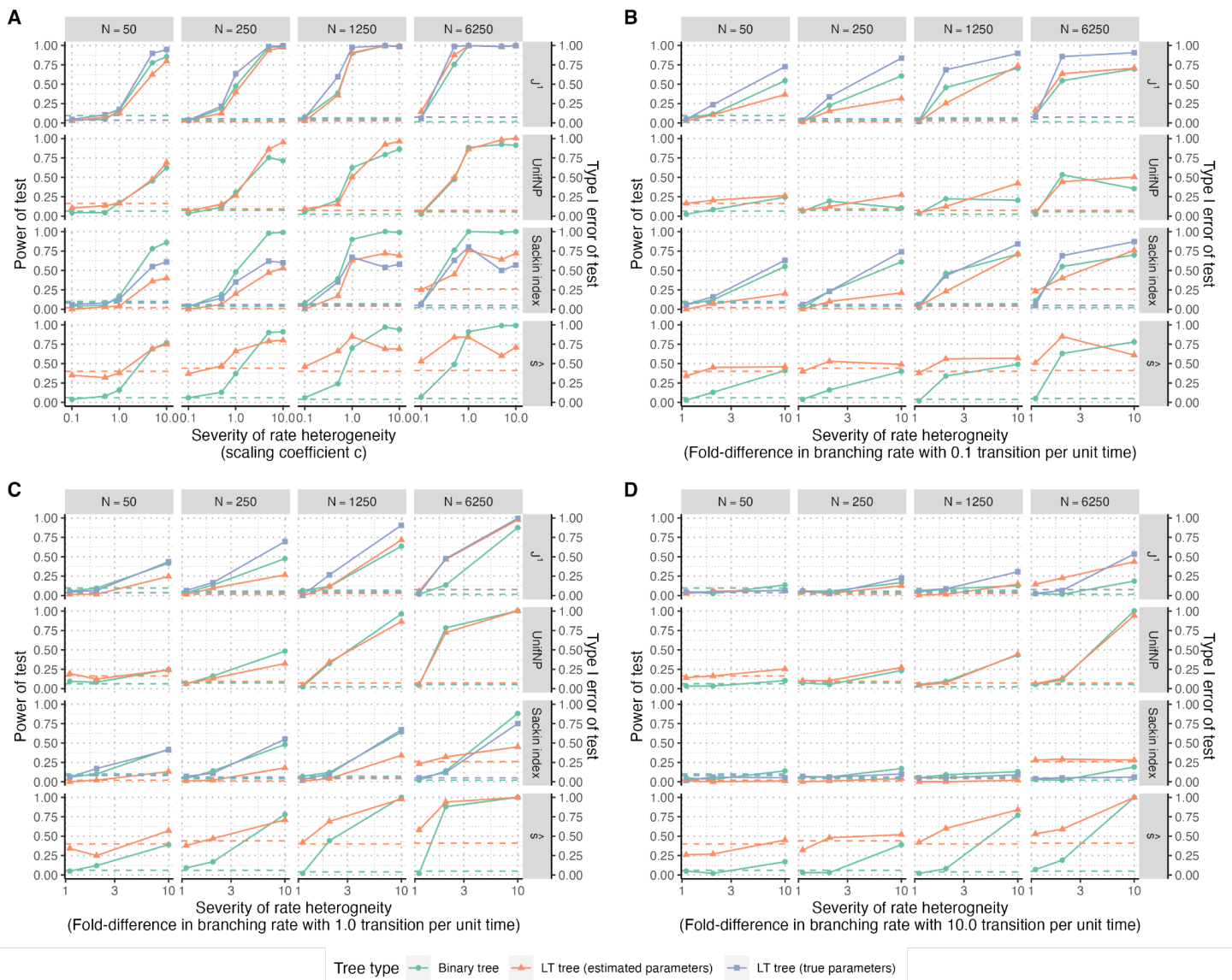


Figure S3. Schematic representation of the four tests based on  $\hat{s}$ ,  $J^1$ , the Sackin index, and UnifNP of the examined tests for tree balance.



**Figure S4**

Performance of  $J^1$ , UnifNP, Sackin index and  $\hat{s}$ -based tests on multifurcating lineage tracing trees. The power (solid lines) and type I error rate (dashed lines) are plotted at tree sizes of  $N = 50, 250, 1250, 6250$  for each mode of branching rate heterogeneity: **(A)** continuous branching rate heterogeneity and **(B-D)** discrete branching rate heterogeneity at transition rates of 0.1, 1.0 and 10.0 transitions per unit time, respectively. The lineage tracing process was simulated under relative latency  $t_{lag}^* = 0.5$  and relative editing rate  $r_{edit}^* = 0.5$ . Tests were performed on the binary trees (green) and multifurcating trees transformed by the lineage tracing process (orange and blue). The null distributions for the  $J^1$  statistic and the Sackin index were generated using either the estimated (orange) or true (blue) lineage tracing parameters. A subset of these conditions are shown in Figures 2 and 3.

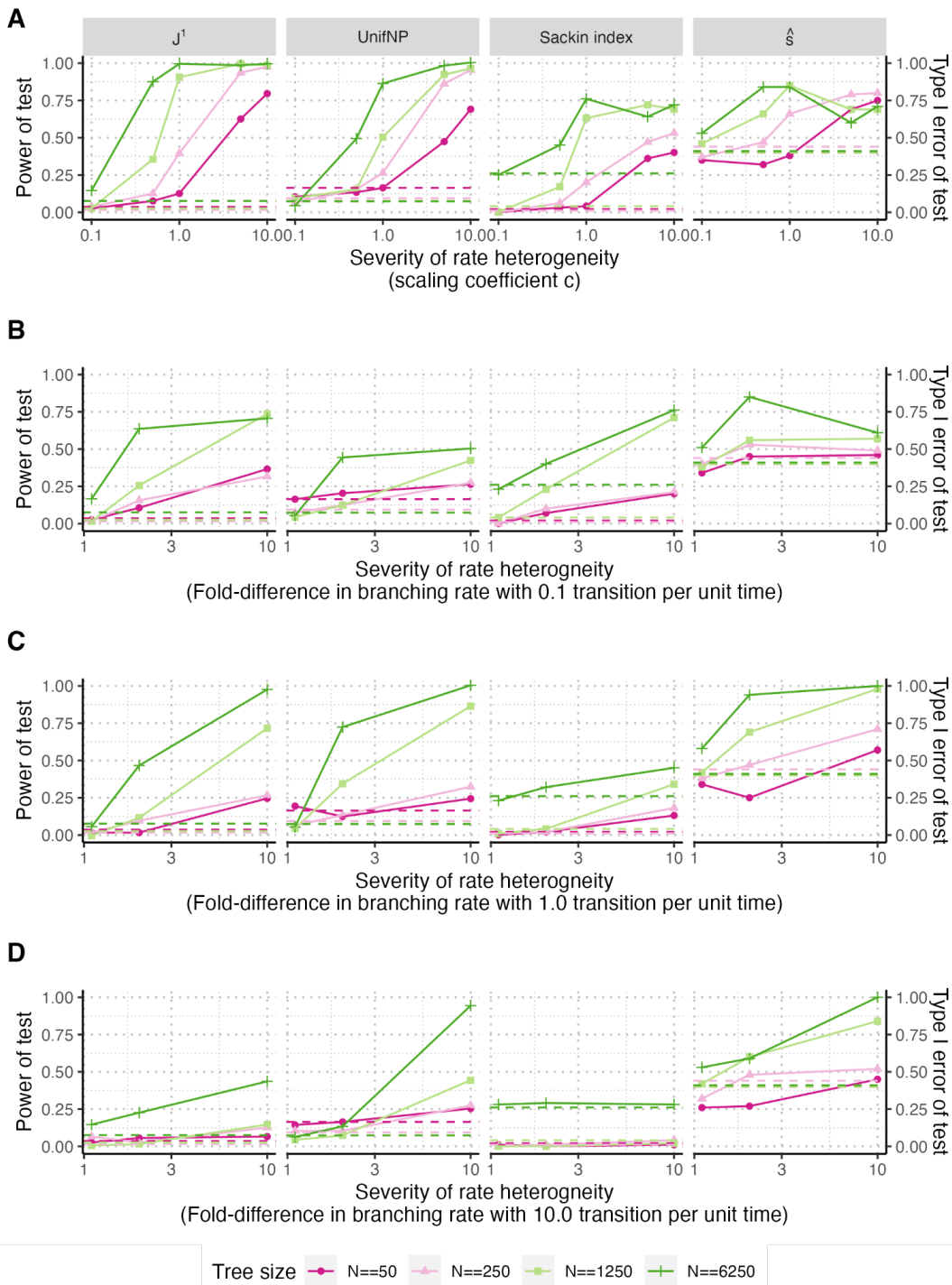


Figure S5.

The effect of tree size on the power of  $J^1$ , UnifNP, Sackin index and  $\hat{s}$ -based tests. The power (solid lines) and type I error rate (dashed lines) of the four tests are plotted at tree size  $N = 50, 250, 1250, 6250$  for each mode of branching rate heterogeneity: **(A)** continuous branching rate heterogeneity and **(B-D)** discrete branching rate heterogeneity at transition rates of 0.1, 1.0 and 10.0 transitions per unit time, respectively. The tests were applied to multifurcating trees and the null distributions of the  $J^1$  statistic and the Sackin index were generated using estimated lineage tracing parameters.

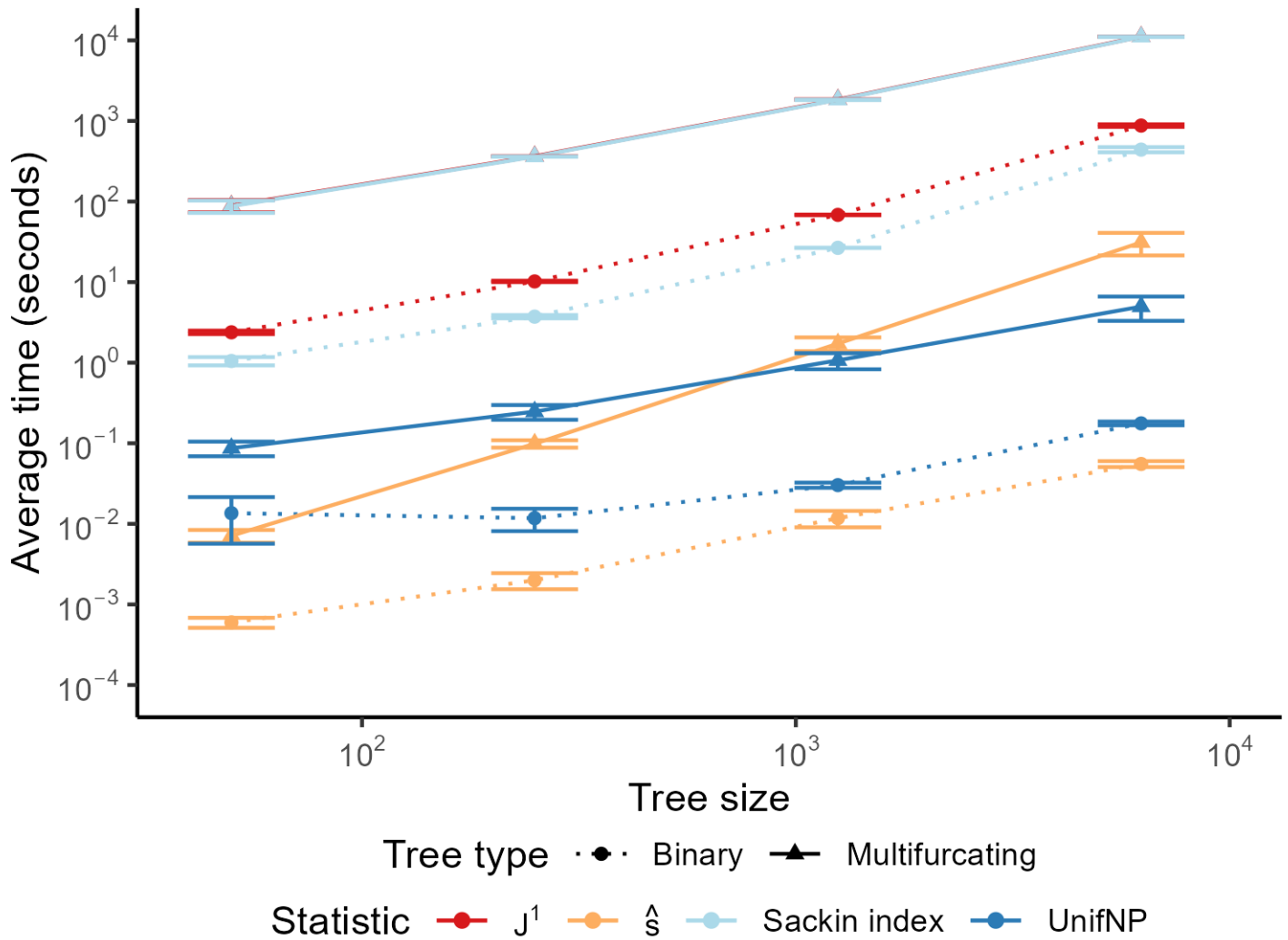
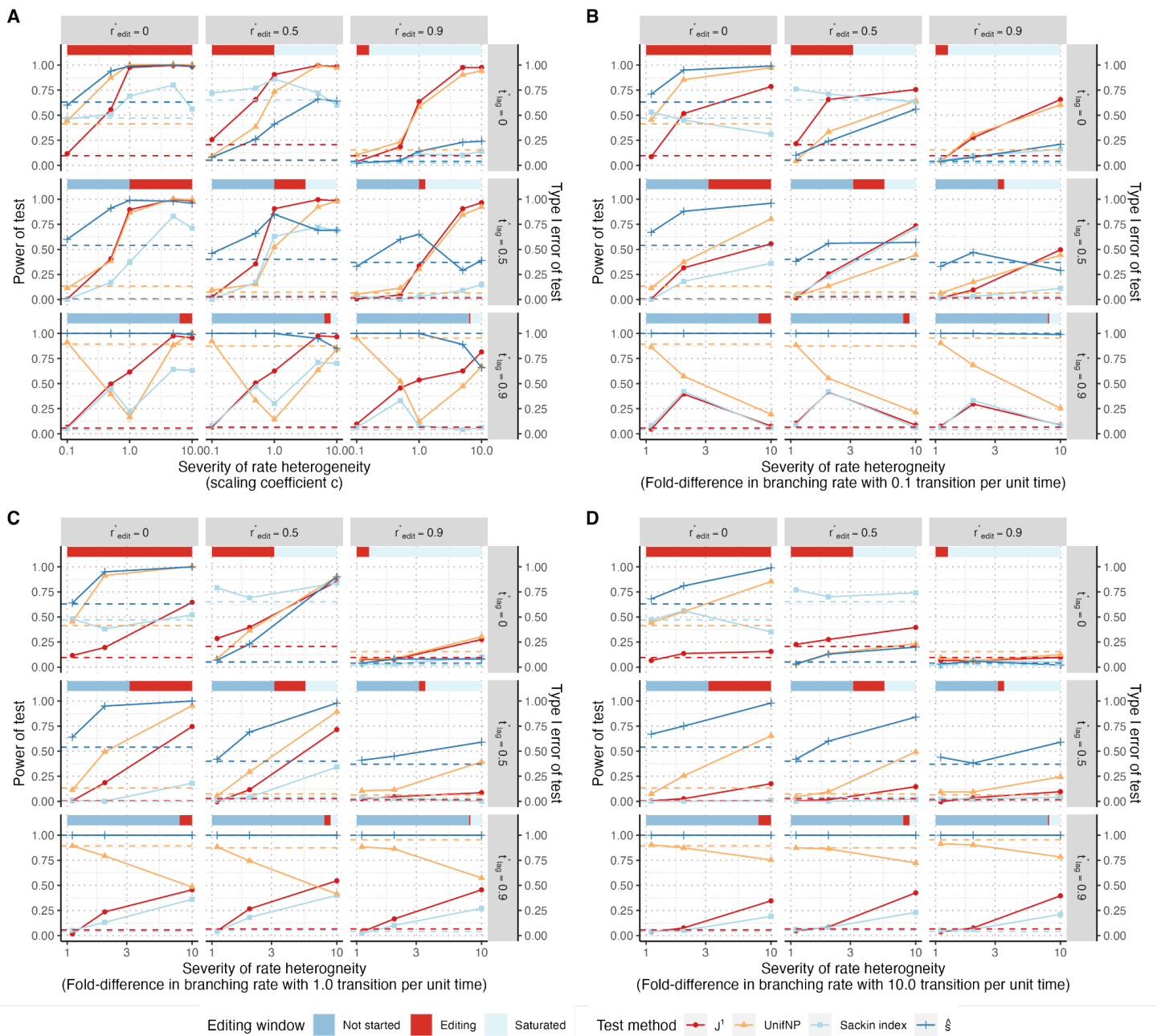


Figure S6.

Computation time benchmarking for the four tests on binary and multifurcating trees. The computation time was averaged across 10 trees (with lineage tracing parameters and the null distribution calculated from scratch). Bars represent the 95% confidence interval of the mean. The multifurcating  $J^1$  computation time is nearly identical to the Sackin index computation time, and is not clearly visible.





**Figure S7.**

Robustness of  $J^1$ , UnifNP, Sackin index and  $\hat{s}$ -based tests to diverse lineage tracing parameters. The power (solid lines) and type I error rate (dashed lines) are plotted for each mode of branching rate heterogeneity and a fixed tree size of  $N = 1250$ : **(A)** continuous branching rate heterogeneity and **(B-D)** discrete branching rate heterogeneity at transition rates of 0.1, 1.0 and 10.0 transitions per unit time, respectively. The lineage tracing process was simulated under all combinations of relative latency  $t_{lag}^* = (0, 0.5, 0.9)$  and relative editing rate  $r_{edit}^* = (0, 0.5, 0.9)$ , generating editing windows as marked in the red and blue-colored bars. The null distributions of the  $J^1$  statistic and the Sackin index were generated using estimated lineage tracing parameters.

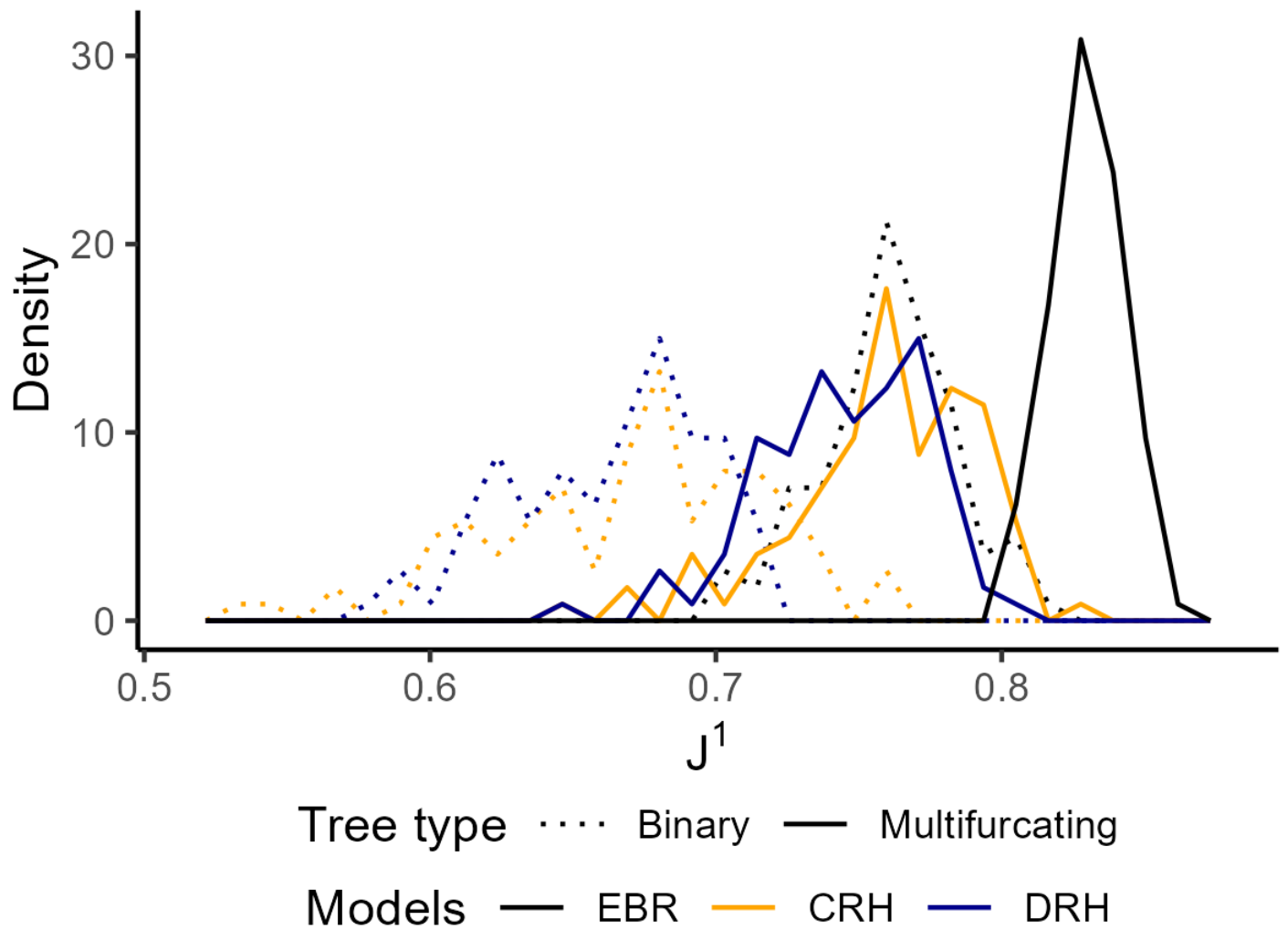


Figure S8.

The empirical distribution of the  $J^1$  statistic under different tree types and branching rate models. The empirical distribution was sampled from 100 trees ( $N=6250$ ) in each model (CRH:  $c=0.5$ , DRH: 10-fold rate change and 1.0 transition per unit time). The multifurcating trees were generated under relative latency  $t_{lag}^* = 0.5$ , relative editing rate  $r_{edit}^* = 0.5$  and barcode length  $k = 20$ .